# NATIONAL ADVISORY COMMITTEE FOR AERONAUTICS

**TECHNICAL NOTE 3372**

## FLIGHT MEASUREMENTS OF BASE PRESSURE ON BODIES OF REVOLUTION WITH AND WITHOUT SIMULATED ROCKET CHAMBERS

By Robert F. Peck

Langley Aeronautical Laboratory
Langley Field, Va.

NACA

Washington
April 1955

NATIONAL ADVISORY COMMITTEE FOR AERONAUTICS

TECHNICAL NOTE 3372

# FLIGHT MEASUREMENTS OF BASE PRESSURE ON BODIES OF REVOLUTION WITH AND WITHOUT SIMULATED ROCKET CHAMBERS[1]

By Robert F. Peck

## SUMMARY

Base pressures were measured in flight on fin-stabilized bodies of revolution with and without rocket chambers and with and without a converging afterbody. The Mach number range covered was between 0.7 and 1.2. Results show that pressures over the center portion of the bases of models with rocket chambers were higher (less suction) than edge pressures, whereas the center base pressures on models without rocket chambers were lower than edge pressures. The effects of rocket chambers on edge pressures were not, in general, as appreciable as the effects on the pressures measured over the center portion of the bases. The results further show that changing from a cylindrical to a convergent afterbody decreased base drag markedly and in this particular case caused the base drag to become negative at Mach numbers below 1.07.

## INTRODUCTION

It has been found that base-pressure drag may have considerable effect on the total-drag characteristics of coasting missiles used in warfare and research models used to determine total-drag characteristics of proposed aircraft. The results of some previous base-drag investigations are presented in references 1 to 5. The Pilotless Aircraft Research Division of the Langley Laboratory is conducting further tests to determine factors affecting base drag.

It has been assumed in the past that an orifice on the annulus of the base of a coasting rocket model provided an accurate measure of base drag. Tests described herein were conducted in 1949 to check the validity of this assumption and, in particular, to determine the effect

[1]Supersedes recently declassified NACA RM L50I28a, 1950.

of a "cold" rocket chamber (with exit at base of model) on pressure over the base of a fuselage with fins. Fuselage configurations used were bodies of revolution and consisted of one configuration with a converging afterbody and three configurations with cylindrical afterbodies.

## MODELS AND TESTS

Configurations used in this investigation are shown in figure 1. All the models were externally the same with the exception of the portion of the body to the rear of the fins. The basic configuration was a cylindrical body 5 inches in diameter with an ogival nose and four stabilizing fins. The body was constructed of wood and had a polished lacquer finish. The fins were made of 0.09-inch-thick duralumin sheet and had rounded leading edges of 0.045-inch radius; the trailing edges were square. Configuration A had a closed flat base, configuration B had a dummy rocket chamber with nozzle exit flush with a flat base, and configuration C had a dummy rocket chamber with nozzle exit 1.2 inches to the rear of the model base. Configuration D had 6.2 inches additional length to the rear of the original base, which converged to a base diameter of 3.3 inches, and had a dummy rocket chamber with nozzle exit flush with the model base. Configurations A, B, and C had fineness ratios of 11.1 and configuration D had a fineness ratio of 12.3. A photograph of configuration D on the booster ready for launching is shown as figure 2.

Pressure measurements were made at two points on each model as shown in figure 1. One of the orifices was located on the center line and the other about 3/8 inch from the circumference of the base of the body (hereinafter referred to as edge orifice). On configurations B, C, and D the center-line orifice was located on the inside of the front bulkhead of the dummy rocket chamber.

Two models of each of the configurations A, B, and C and one model of configuration D were flown. Each of the models was boosted to speed by a fin-stabilized 5-inch lightweight HVAR motor. Base pressures were measured through the use of standard NACA pressure cells and telemeters. Portions of typical telemeter records are shown in figures 3, 4, and 5. Mach number and free-stream static and dynamic pressures were obtained from Doppler radar, SCR 584 radar, and radiosonde data in the manner described in reference 5.

Since the static margin of these models was of the order of 2 to 3 body diameters, they were assumed to have been at or very near zero angle of attack throughout the flights.

The test Reynolds numbers R based on body length are shown plotted against Mach number M in figure 6.

## RESULTS AND DISCUSSION

Results of this investigation are presented in the form of the base pressure minus free-stream static pressure divided by free-stream dynamic pressure $\Delta p/q$ plotted against Mach number in figures 7 to 12. The data obtained from the configurations A, B, C, and D are shown in figures 7 to 10. The average edge-orifice $\Delta p/q$ data from each of the configurations A, B, and C are shown in figure 11. Figure 12 is a summary plot of all the $\Delta p/q$ data obtained in this investigation.

It should be noted that the data from configurations A, B, and C (figs. 7 to 9) appear to be erratic and there is some apparent disagreement between supposedly identical models of the same configuration. Some understanding of these conditions may be gained from an examination of the telemeter records from these models and of the sources of error affecting the results.

The telemeter records of base pressure from models with cylindrical afterbodies at Mach numbers between 0.7 and 1.2 were very oscillatory. A portion of a typical record obtained from a model with a cylindrical afterbody at Mach numbers near 1.0 is shown in figure 3. The irregularity of the oscillations and of the mean line faired through them indicates that this is not a pure resonant condition of the pressure-measuring system even though the indicated high-frequency oscillations are of approximately the same frequency as the resonant frequency of the pressure-cell and tubing combination. A comparison with a portion of the same record obtained at Mach numbers of the order of 0.3 to 0.4 (fig. 4) indicates that oscillations as severe as those shown in figure 3 were not recorded throughout the model flights. Records of body side pressures obtained through the Mach number range 0.7 to 1.8 from other models equipped with similar pressure-measuring systems (unpublished data) show no appreciable oscillations. The foregoing factors, considered together, indicate that there were relatively large pressure fluctuations at the bases of configurations A, B, and C at Mach numbers between 0.7 and 1.2 which were probably caused by strong turbulence somewhere in the wake. The data presented in figures 7 to 9 were obtained from a faired line drawn through the resulting oscillatory records.

The maximum disagreement between corresponding $\Delta p/q$ data from two identical models is approximately 0.06 and occurs at subsonic speeds between models 1 and 2 of configuration A. Such disagreement in $\Delta p/q$ at subsonic speeds may be caused by an additive combination of possible

experimental errors of the order of 1 percent in measurement of absolute base pressure and free-stream static pressure. Of these, only the errors in absolute base-pressure measurements would affect the differences in $\Delta p/q$ data between two orifices on a given model.

It is believed that the summary curve, figure 12, describes the qualitative differences in data from configurations A, B, and C since the same conclusions may be made upon examination of data from models 1, models 2, or the average data from them.

Tests made on configuration D (model with convergent afterbody) resulted in a telemeter record and $\Delta p/q$ data, shown in figures 5 and 10, respectively, which were far less fluctuant than those obtained from configurations A, B, and C. This result may indicate that there is less severe turbulence behind the body with the convergent afterbody than behind the configurations with cylindrical afterbodies.

It should be noted that the indicated oscillations shown in figures 3 and 5 are not quantitatively indicative of the turbulence frequency or intensity because the indicated high-frequency oscillations are the same frequency as the natural frequency of the pressure-measuring systems, as mentioned previously. Examination of the portion of telemeter record shown in figure 3 might lead one to conclude that the turbulence at the edge-orifice station was more severe than that at the center. Examinations of all the records, however, indicated no consistent trend in this respect.

The edge-orifice data summarized in the curves of figure 11 indicate that differences in edge-orifice pressures for configurations A, B, and C were not consistent throughout the Mach number range nor in general as appreciable as the differences in center-orifice pressures (fig. 12).

The summary plot (fig. 12) indicates that the addition of a rocket chamber with its opening flush with the base of the model reduces the suction on the center portion of the model base from a value greater than to a value lower than that measured near the circumference. No suitable explanation of these indicated phenomena is known. A similar small reduction in base suction, however, has been noted in unpublished data on a similar configuration tested in the Langley 9-inch supersonic tunnel at a Mach number of 1.92.

The curves shown in figure 12 further indicate that moving the rocket chamber rearward (configuration C) in relation to the base of the model reduces the suction on the center portion of the model an additional amount. This might be explained by small changes in the flow due to the slight change in the external characteristics of the

model or by the difference in the position, relative to the base, along the wake in which the pressure was measured. Since the edge-orifice pressure was not appreciably affected by this change in configuration (except near $M = 1.0$), the latter explanation seems more logical.

The data from configuration D (figs. 10 and 12) show that suction over the center portion of the fuselage with a converging afterbody and with a rocket chamber was less than the suction at the edge. This is in agreement qualitatively with data from configurations B and C. The base pressure coefficients $\Delta p/q$ obtained from configuration D further indicate that the base drag of the fuselage with the converging afterbody was markedly less than the base drag of a comparable fuselage with a cylindrical afterbody. The difference in base suction (or base drag) caused by the change in afterbody at Mach numbers above 1.0 agrees in direction and roughly in magnitude with data presented in reference 1 which shows data obtained on similar models, but without fins, at a Mach number of 1.5. It may also be noted that the $\Delta p/q$ values obtained are positive (negative drag) at Mach numbers below 1.07 for the inside orifice and 1.01 for the edge orifice in the Mach number range covered. Positive base pressure coefficients have also been measured on other models (ref. 1 and unpublished data). Schlieren pictures in reference 1 indicate that positive base pressure measured at a Mach number of 1.5, on a model with an afterbody of comparatively high convergence and having turbulent boundary layer, resulted from a compression through a shock wave just ahead of the base of the model. In the tests of reference 1, a "base shock" (rather than an expansion wave as in the case of cylindrical afterbodies), accompanied by the usual wake shock, appeared on all models with convergent afterbodies and turbulent boundary layer. This base shock increased in intensity as the afterbody convergence was increased, until, as in the case of the model on which positive base pressure was measured, the base shock was the predominant one. A similar condition may have caused this positive base pressure measured at low supersonic speeds on configuration D.

## CONCLUSIONS

Base-pressure measurements were made on several fin-stabilized bodies of revolution. The data obtained indicate the following conclusions:

1. The presence of a rocket chamber with exit flush with the base of a fuselage having a cylindrical afterbody decreased the suction over the center portion of the base to a value lower than that near the circumference as compared to a similar closed-base model where the center suction was greater than that measured near the circumference.

2. Moving the rocket exit to the rear of the base of a fuselage having a cylindrical afterbody resulted in a measured suction over the center portion which was lower than that measured on a similar model with a rocket-chamber exit flush with the base.

3. The base pressures measured near the circumference of the fuselages with a cylindrical afterbody were, in general, not affected as appreciably by the rocket in either position as were the pressures measured on the center line.

4. The pressure over the center portion of the bases of fuselages with rocket chambers was less negative than pressures near the circumference in the case of fuselages with either converging or cylindrical afterbodies.

5. Adding a convergent afterbody to a cylindrical fuselage decreased base drag markedly and in this particular case caused this base drag to become negative at Mach numbers below 1.07 (in the Mach number range covered).

Langley Aeronautical Laboratory,
National Advisory Committee for Aeronautics,
Langley Field, Va., September 20, 1950.

## REFERENCES

1. Chapman, Dean R., and Perkins, Edward W.: Experimental Investigation of the Effects of Viscosity on the Drag and Base Pressure of Bodies of Revolution at a Mach Number of 1.5. NACA Rep. 1036, 1951. (Supersedes NACA RM A7A31a.)

2. Perkins, Edward W.: Experimental Investigation of the Effects of Support Interference on the Drag of Bodies of Revolution at a Mach Number of 1.5. NACA TN 2292, 1951. (Supersedes NACA RM A8B05.)

3. Faro, I. D. V.: Experimental Determination of Base Pressures at Supersonic Velocities. Bumblebee Rep. No. 106, The Johns Hopkins Univ., Appl. Phys. Lab., Nov. 1949.

4. Chapman, Dean R.: An Analysis of Base Pressure at Supersonic Velocities and Comparison With Experiment. NACA Rep. 1051, 1951. (Supersedes NACA TN 2137.)

5. Morrow, John D., and Katz, Ellis.: Flight Investigation at Mach Numbers From 0.6 to 1.7 To Determine Drag and Base Pressures on a Blunt-Trailing-Edge Airfoil and Drag of Diamond and Circular-Arc Airfoils at Zero Lift. NACA RM L50E19a, 1950.

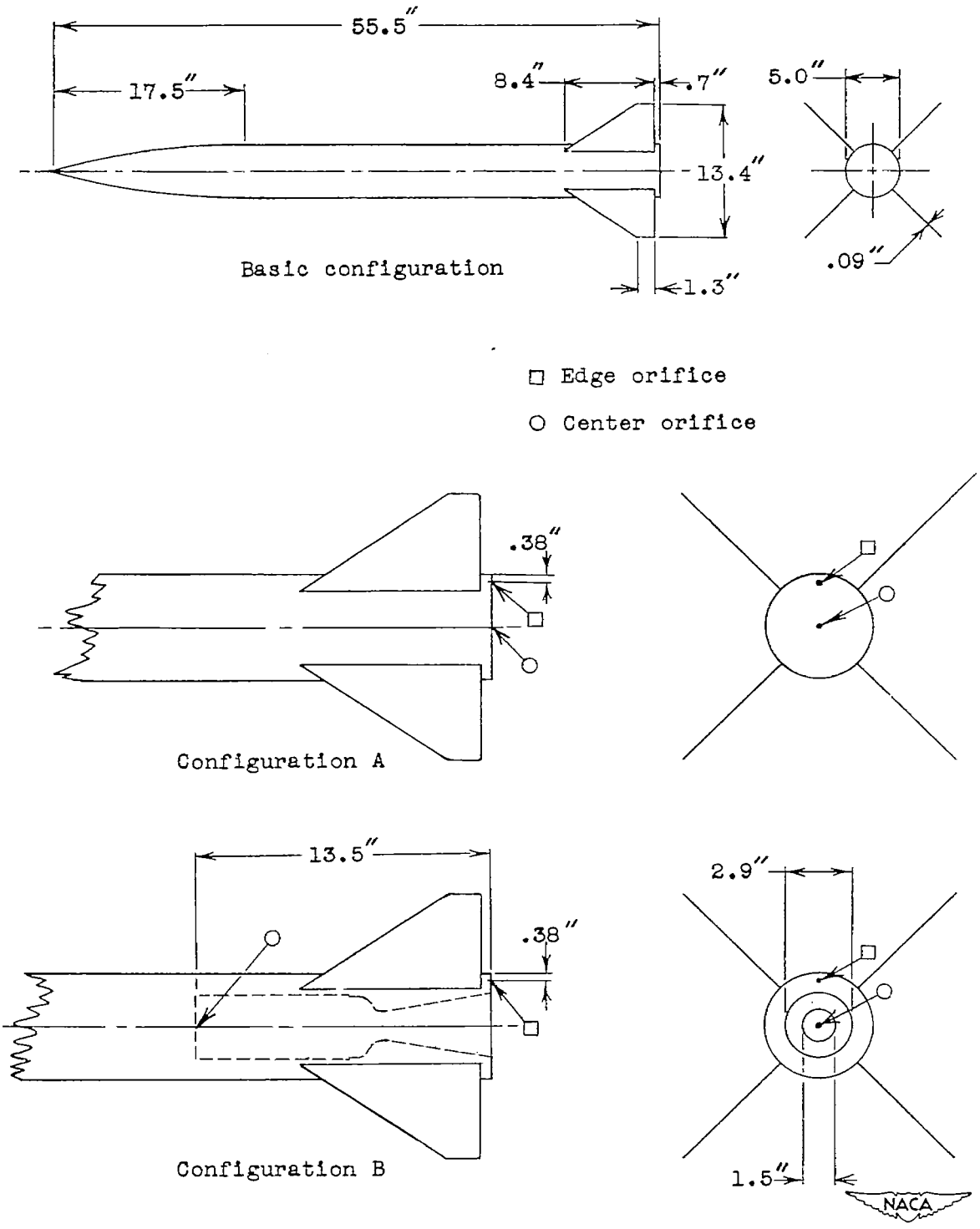


Figure 1.- Sketch of models used in tests.

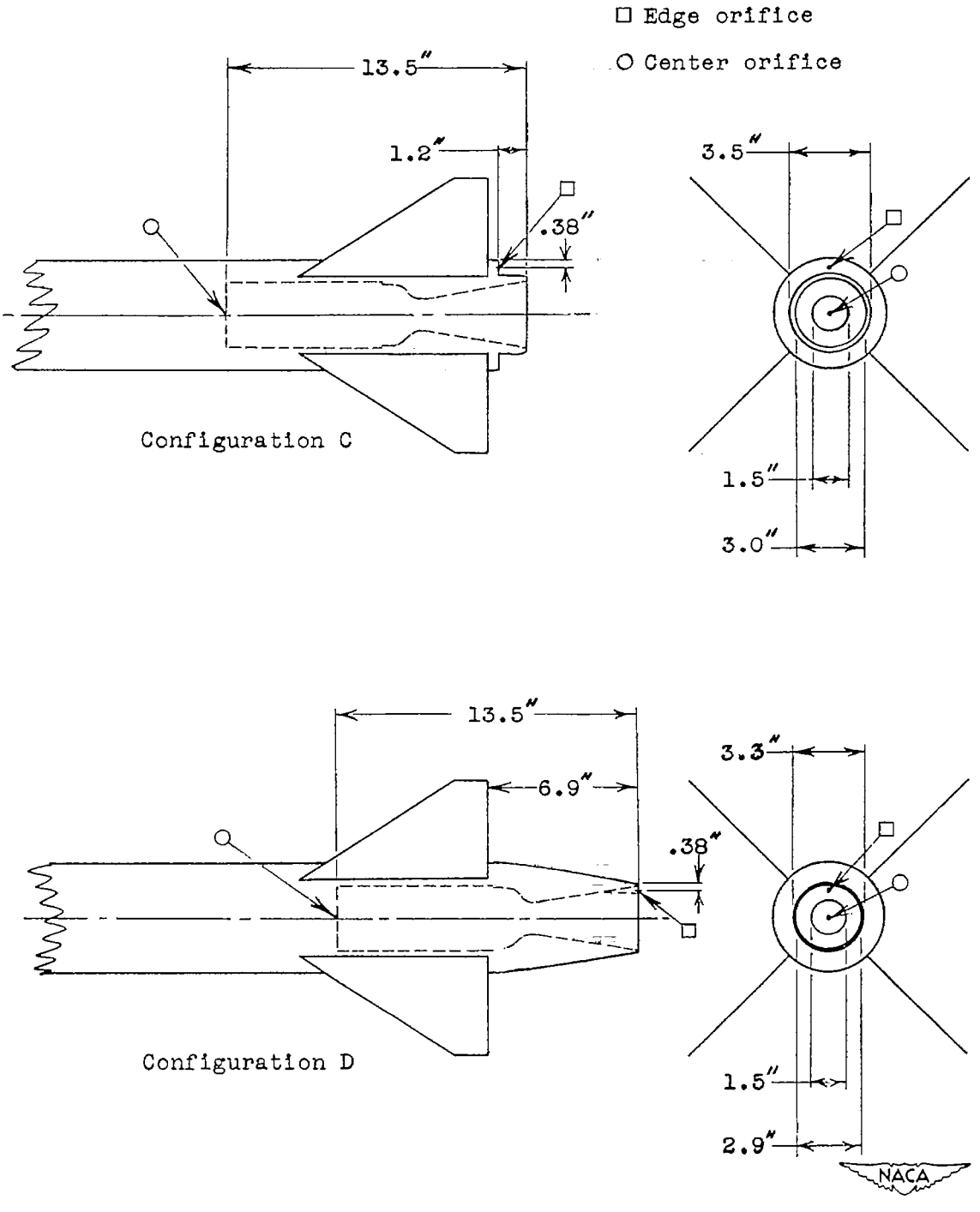


Figure 1.- Concluded.

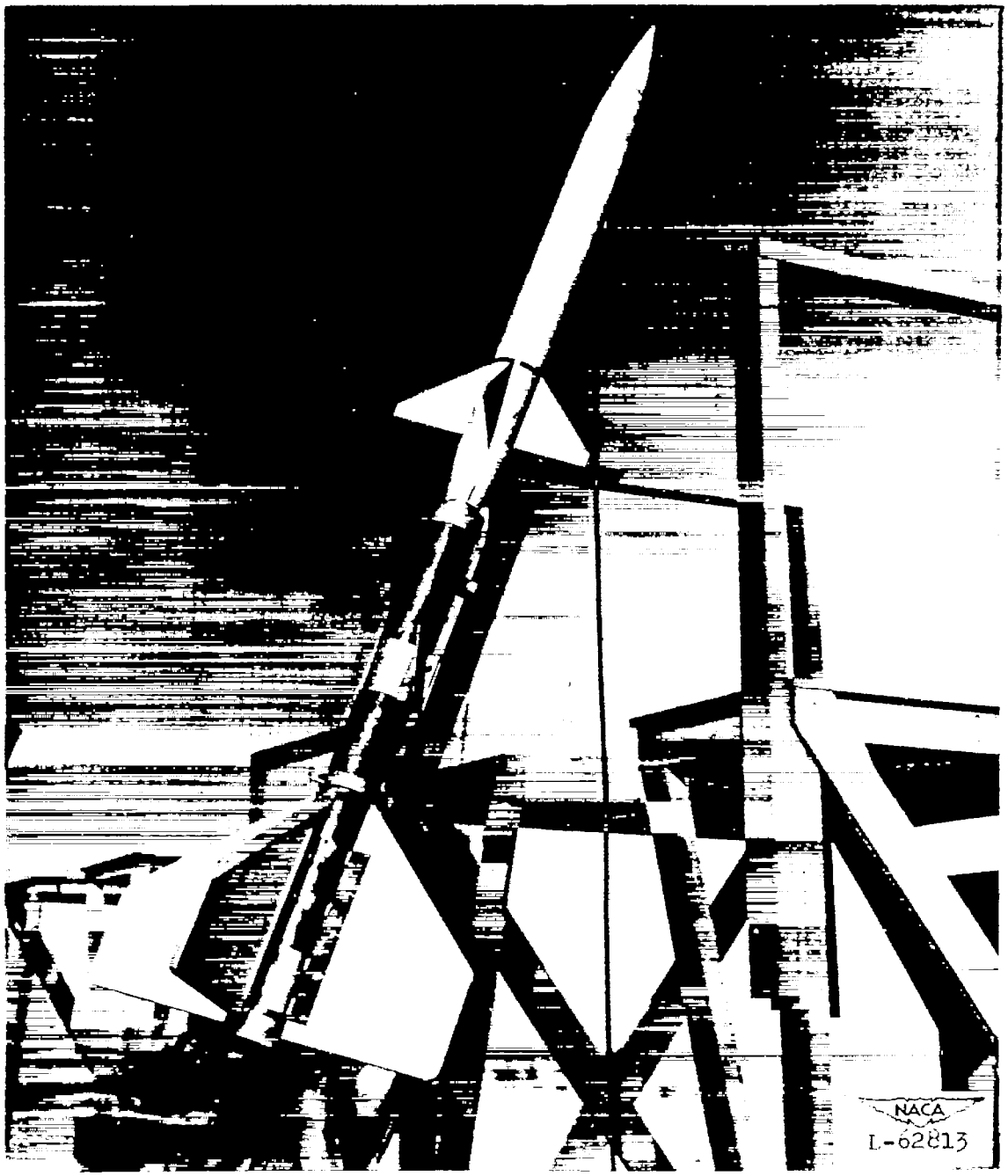


Figure 2.- Configuration D on booster ready for launching.

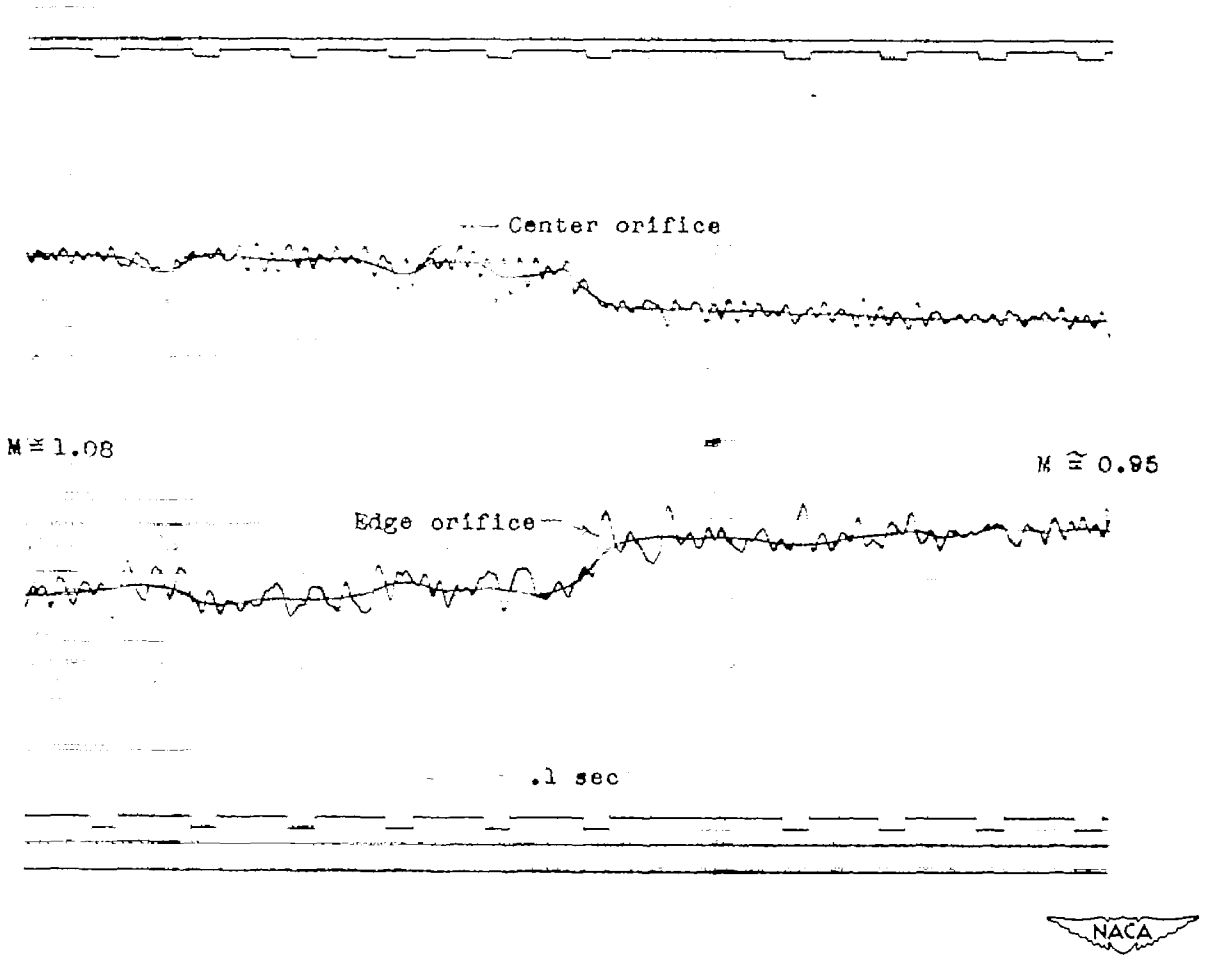


Figure 3.- Portion of telemeter record of variation of base pressure with time from configuration A, model 2, near M = 1.0.

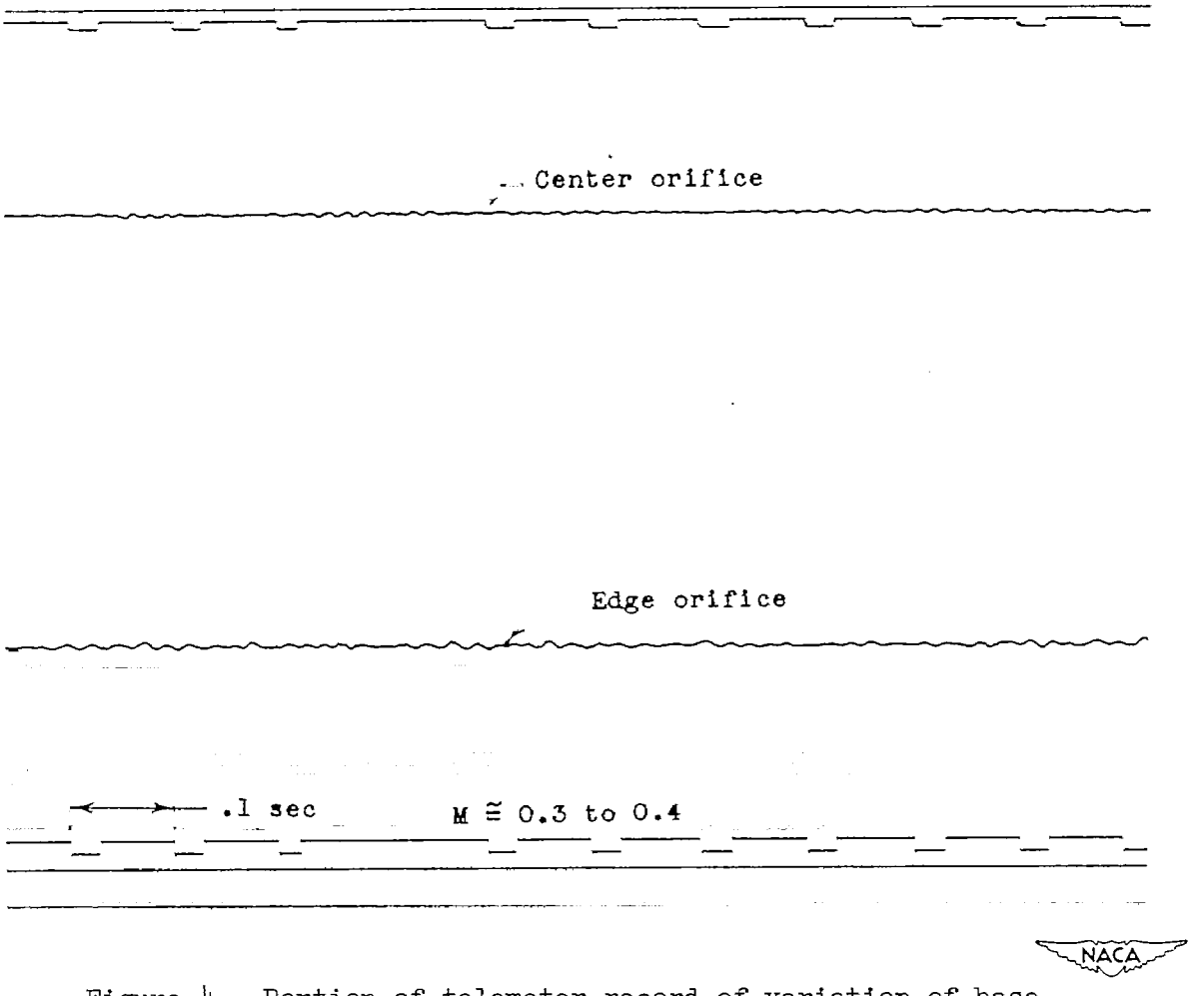


Figure 4.- Portion of telemeter record of variation of base pressure with time from configuration A, model 2, at very low Mach numbers.

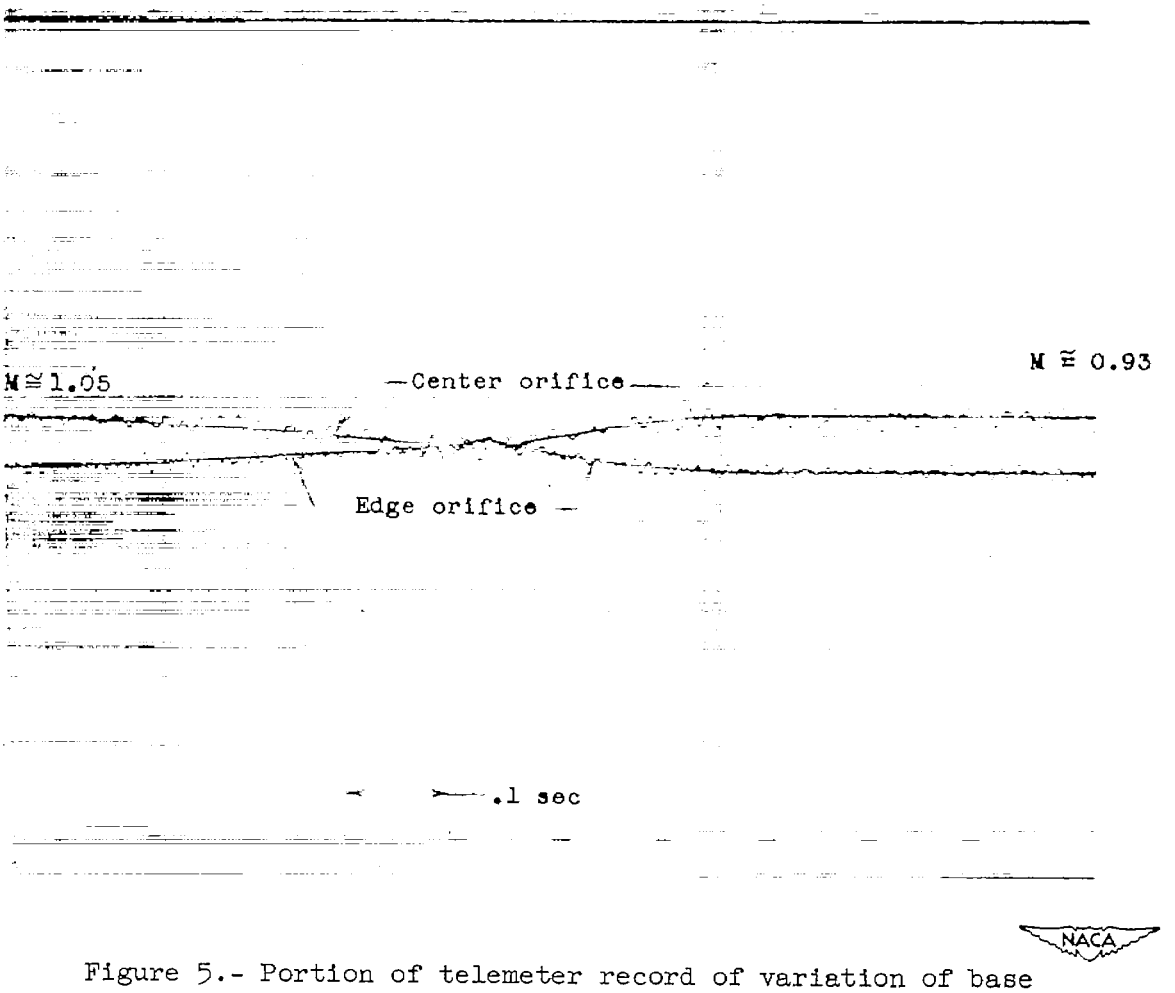


Figure 5.- Portion of telemeter record of variation of base pressure with time from configuration D with a converging afterbody.

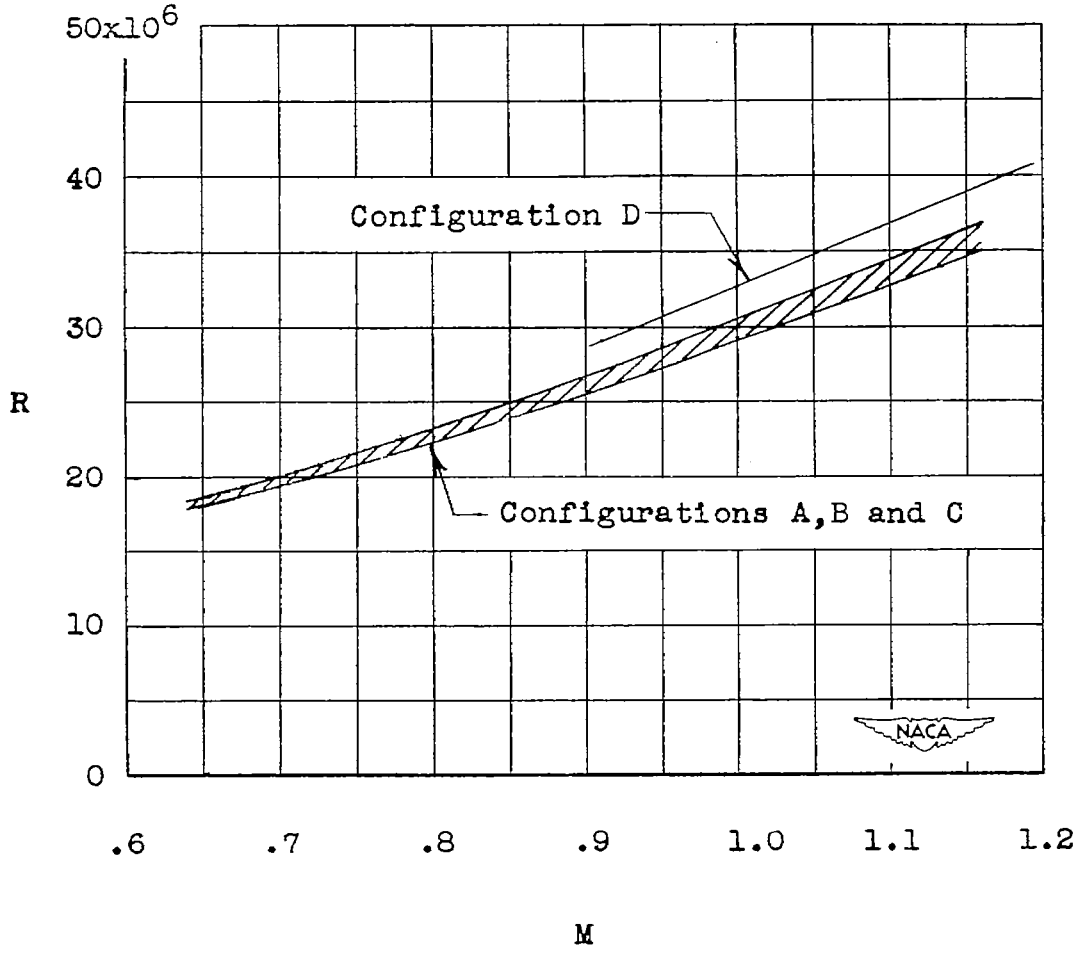


Figure 6.- Variation of test Reynolds number R with Mach number M.

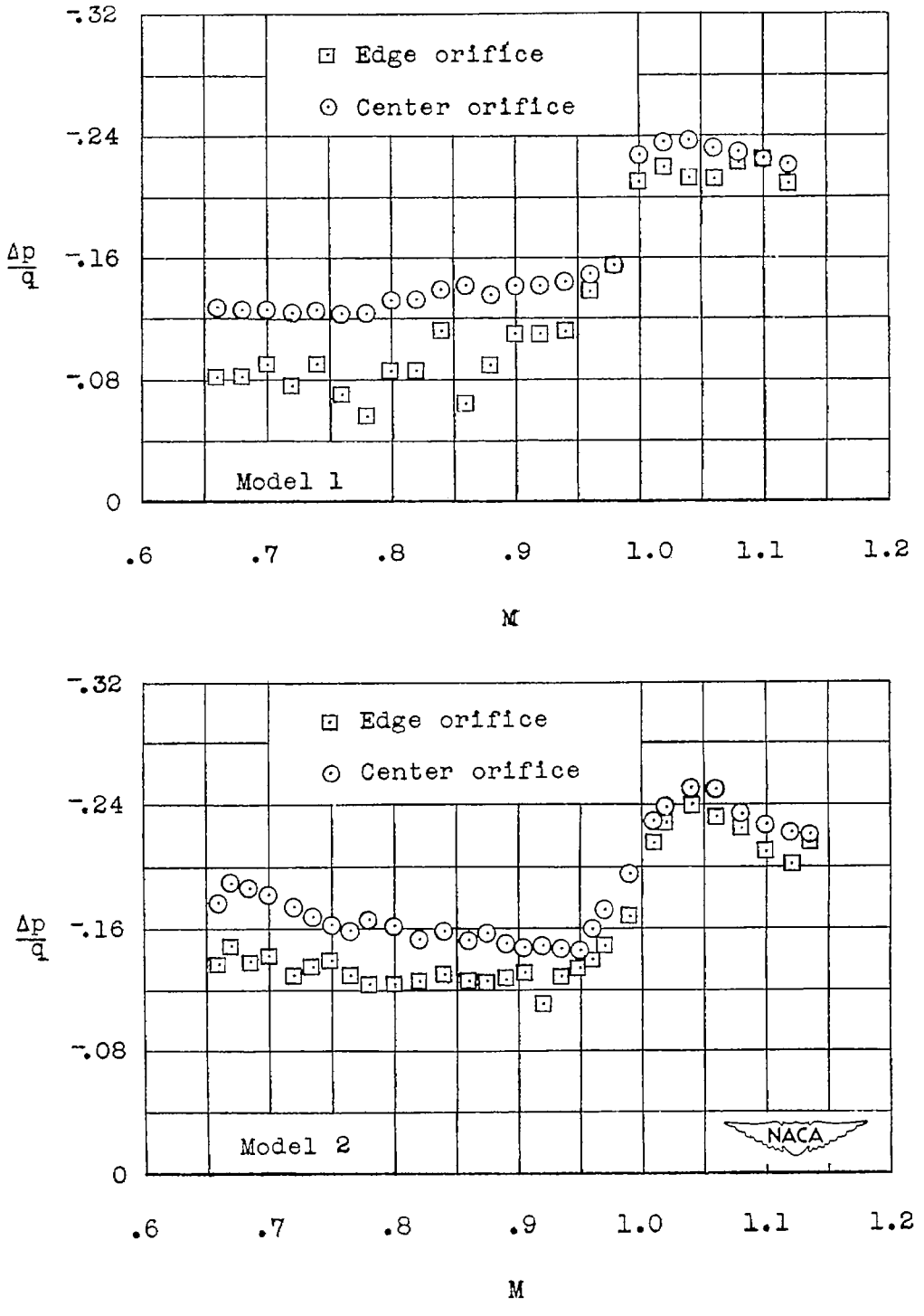


Figure 7.- Variation of base pressure coefficient $\frac{\Delta p}{q}$ with Mach number M as measured on configuration with flat closed base (configuration A).

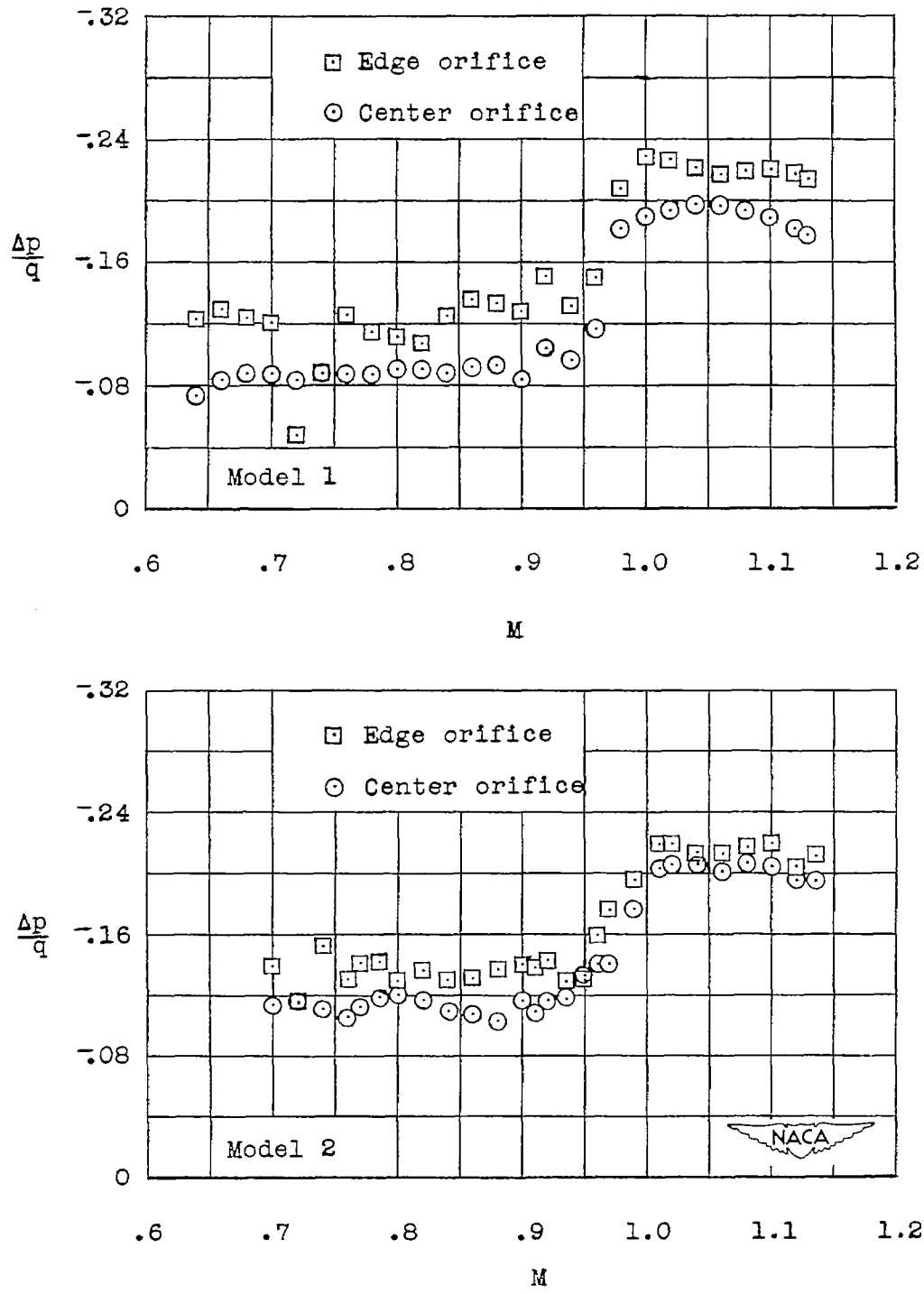


Figure 8.- Variation of base pressure coefficient $\frac{\Delta p}{q}$ with Mach number M as measured on configuration with rocket-nozzle exit flush with base (configuration B).

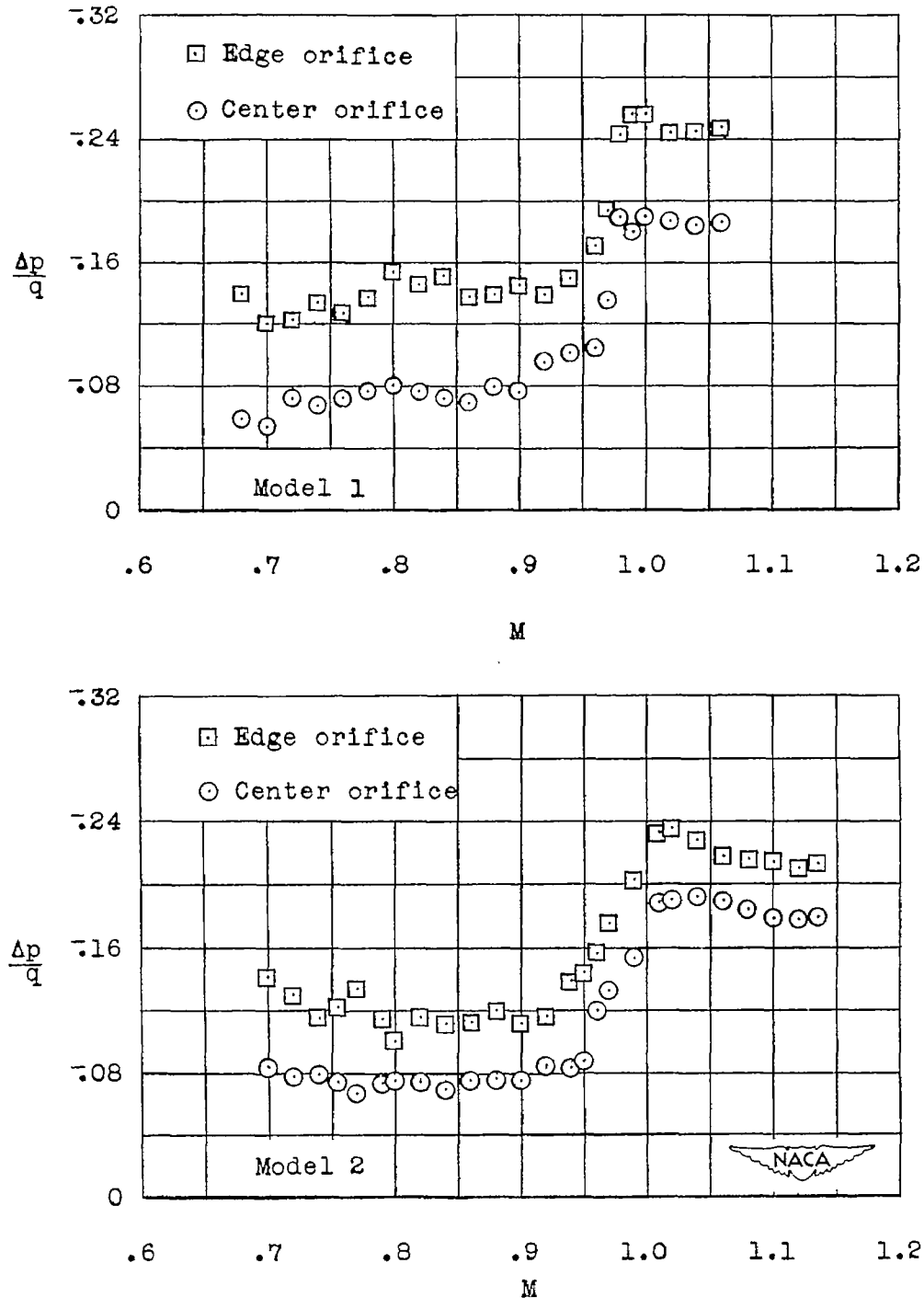


Figure 9.- Variation of base pressure coefficient $\frac{\Delta p}{q}$ with Mach number M as measured on configuration with rocket-nozzle exit 1.2 inches aft of model base (configuration C).

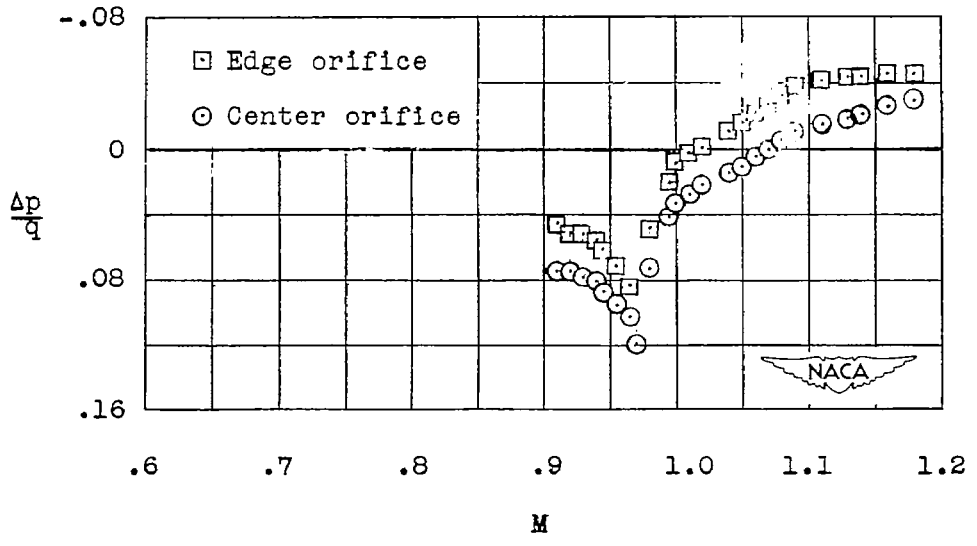


Figure 10.- Variation of base pressure coefficient $\frac{\Delta p}{q}$ with Mach number M as measured on configuration with convergent afterbody (configuration D).

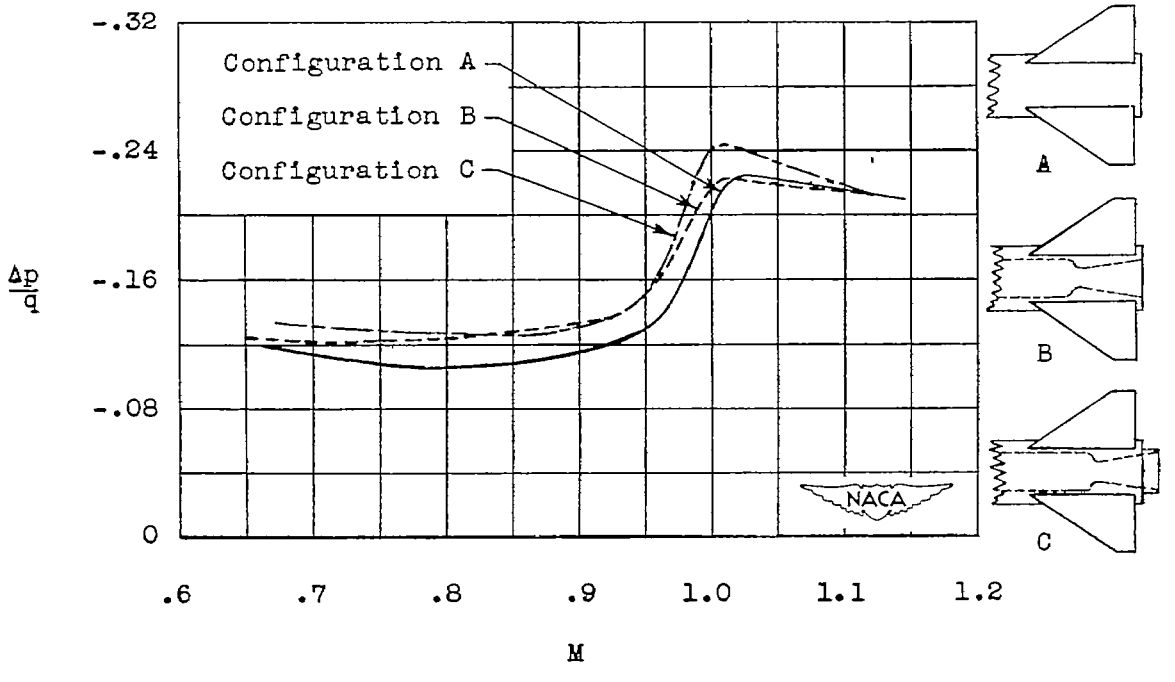


Figure 11.- Variation of average edge-orifice base pressure coefficient $\frac{\Delta p}{q}$ with Mach number M from each of configurations A, B, and C.

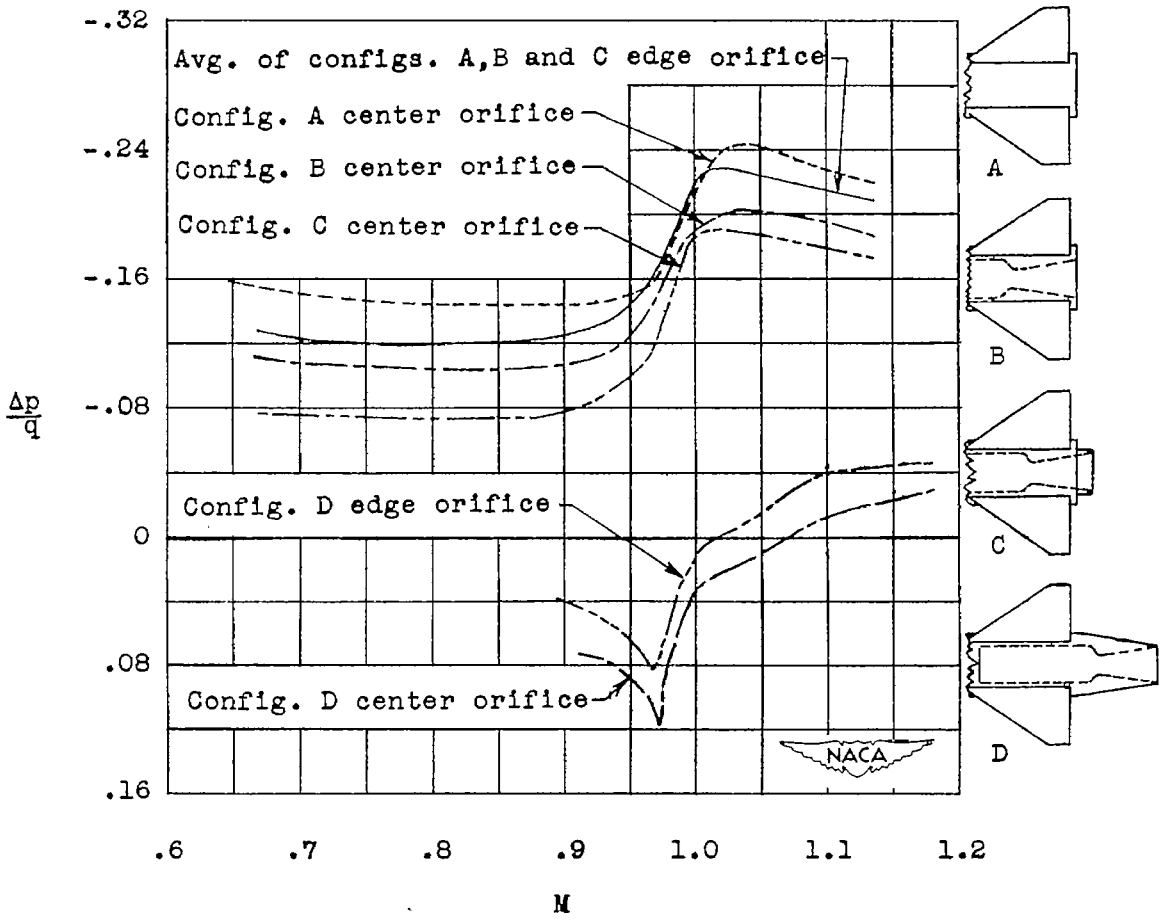


Figure 12.- Summary of base-pressure-coefficient $\frac{\Delta p}{q}$ data from configurations A, B, C, and D.